The emerging role of receptor trafficking in signalosome formation and sustained long-term Wnt/β-catenin signaling

Fiete Haack, Kevin Burrage, Adelinde Uhrmacher

2025

Abstract

Despite its central role in development, cell homeostasis, and cancer, the mechanisms that induce and transduce Wnt signaling, particularly the role and impact of receptor internalization, have been under discussion for almost two decades. To integrate seemingly contradictory experimental observations into a coherent explanatory framework, we developed a mechanistic computational model that dissects the spatiotemporal regulation of canonical Wnt signaling. For this, a newly optimized multi-level rule-based modeling and simulation approach is employed to describe and simulate the compartmental distribution of extracellular, intracellular, and membrane-associated signaling molecules, as well as a concise representation of the receptor life cycle, including internalization, degradation, and recycling processes.

Our simulations show that cells can compensate for the partial immobilization of receptor complexes by internalization (the movement of molecules into the cell) and rapid recycling (the return of these molecules to the cell membrane). This process ensures the formation of larger and more stable protein-receptor complexes (signalosomes) and the continuation of the signaling process. Our results imply that degradation and recycling are essentially required for stable, long-term signaling (in terms of beta-catenin aggregation). This process is often overlooked in its importance for stable, long-term signal maintenance, and it provides a possible explanation for why excessive signal activation in cancer cells is highly dependent on internalization and recycling processes. Having integrated the concept of rebinding (the process by which proteins return to their original location) and residence time (how long a protein stays in a particular location), the model illustrates the pivotal role of ordered membrane domains (lipid rafts) in the recruitment of proteins such as DVL (Disheveled) to the membrane and their aggregation. This study highlights the complex interplay of cellular processes involved in Wnt signaling, including lateral diffusion, internalization, recycling, and the role of ordered membrane domains. Integrating

such a multitude of experimental measurements based on varying cell lines/tissues, experimental approaches, and treatments into a simulation model enables comprehensive and in-depth insights into the mechanistic regulation of canonical Wnt signaling, which will open up new possibilities for modulating Wnt signaling in disease contexts.

1 Introduction

The Canonical Wnt pathway is an evolutionarily conserved cell-cell signaling cascade that crucially controls proliferation, migration, and cell-fate decisions in development and adult tissue homeostasis [1, 2, 3] In its aberrant form, canonical Wnt signaling is critically involved in the pathogenesis of various diseases, such as neurodegenerative disorders, metabolic syndromes, autoimmune diseases, and cancer [4, 5].

In canonical Wnt signaling, the central regulatory step is the stabilization and nuclear translocation of the transcriptional co-activator β-catenin (Catenin β-1). Under basal conditions, i.e., when Wnt ligands are absent, β-catenin is continuously targeted for degradation by the destruction complex. This multiprotein complex includes the scaffold components Adenomatous Polyposis Coli (APC) and Axis Inhibition Proteins 1 and 2 (AXIN1/2), which recruit β-catenin, as well as the serine/threonine kinases Casein Kinase I α (CK1α) and Glycogen Synthase Kinase 3β (GSK3β) [6, 7]. These kinases sequentially phosphorylate β-catenin, which induces its ubiquitination and subsequent proteasomal degradation [8, 9]. Canonical Wnt signaling is initiated when Wnt ligands bind to their cell-surface target receptors Frizzled (FZD) and low-density lipoprotein receptor-related protein 5 and 6 (LRP). Ligand receptor binding induces the recruitment of Dishevelled (DVL) to the membrane and clustering of receptor protein into membrane microdomains enriched in cholesterol and caveolin-1 (so-called caveolae) oligomerization [10, 11]. These membrane regions promote signalosome assembly — a large complex, favoring LRP6 phosphorylation at multiple PPPSP motifs [12, 13, 14]. LRP6 phosphorylation creates docking sites for Axin, displacing it from the cytoplasmic destruction complex, hence inducing stabilization and nuclear translocation of the target protein β-catenin to regulate target gene transcription as part of a larger transcriptional complex [15, 13, 16].

Recent studies and comprehensive reviews emphasize that membrane trafficking and receptor dynamics are not passive background processes but central regulators of Wnt signal strength, duration, and spatial patterning [17, 18, 19]. A major axis of regulation is receptor and ligand internalization by multiple endocytic routes (clathrin-mediated, caveolin-dependent, macropinocytosis, and other clathrin-independent processes) [20, 21, 22]. Whether endocytosis potentiates or attenuates signaling appears to be context- and cargo-dependent, and is still under discussion [23, 24]. Both positive and negative roles have been reported: Ubiquitin ligases (e.g., ZNRF3/RNF43) and RSPO proteins induce FRZ/LRP6 endocytosis and membrane clearance through clathrin-dependent

internalization, linking signal amplitude to trafficking by controlling cell surface receptor abundance [25, 26, 27, 28]. On the contrary Wnt/FRZ/LRP6 signalosome is internalized through a caveolin-dependent (caveolae-mediated) endocytic route that is known to promote signal transduction: Several studies demonstrate, that disruption of Caveolin-1 or caveolae formation blocks LRP6 internalization and downstream β-catenin activation, underscoring that caveolar uptake is essential for sustained canonical Wnt signaling (eg. [29, 30, 31, 32]).

However, even though the vital role of internalization on Wnt signaling has been manifested by various studies over the last decade, the impact of receptor trafficking and, in particular, receptor recycling has been mostly neglected so far and remains elusive for Wnt signaling [24]. Numerous studies suggest that receptor trafficking plays a beneficial role in various signaling pathways, where continuous rounds of endocytosis and recycling protect receptors from degradation (e.g., [33, 34, 35]). Further receptor trafficking may amplify signal transduction by concentrating ligands and downstream adaptors in endosomes, which prolongs kinase activity (e.g., EGFR, β-adrenergic receptors), while endosomal transport can induce receptor sorting, based on distinct lipid environments [36, 37, 38, 39]. Further, some experimental studies already imply a more central role of receptor trafficking in canonical Wnt signaling than previously anticipated [30, 40].

To explore whether the rapid recycling of raft-associated receptor complexes might also play a beneficial role in Wnt signaling, as recently discussed for other signaling pathways (see above), we developed a mechanistic computational model that dissects the spatiotemporal regulation of canonical Wnt signaling on a quantitative level. Our quantitative modeling and simulation approach is designed to complement traditional experimental studies and conceptual reviews of Wnt pathway dynamics [5, 19]. Existing reviews synthesize extensive experimental findings into coherent but primarily qualitative conceptual models and typically offer little quantitative analysis. By contrast, simulation studies - such as [41, 42, 43] - are well suited to advancing quantitative understanding. Here, we use a simulation framework as a focal point to integrate diverse knowledge sources into a qualitatively and quantitatively coherent picture, enabling us to refine, extend, or even revise current hypotheses about how the receptor life cycle shapes Wnt signaling.

Therefore, we developed a simulation model that integrates diverse data sources, qualitative concepts, and hypotheses about mechanisms into a unified quantitative framework. This enables systematic exploration of existing hypotheses and provides a more coherent and comprehensive understanding of the membrane trafficking and receptor dynamics underlying canonical Wnt signaling.

Due to its central role in numerous biological processes and cellular regulations, as well as in its aberrant form, in cancer development, the Wnt signalling pathway has been the subject of various simulation models [44]. However, membrane dynamics have only been considered in a few models so far [45, 46, 47, 41, 48]; none of them comprises an extensive, pathway-specific representation of receptor trafficking in Wnt signaling. Modeling the receptor life

cycle, including receptor/protein complex formation, ligand - or raft-induced internalization, recycling, and intracellular sorting, poses a major challenge for computational representations of canonical Wnt signaling. These processes, together with the resulting spatial heterogeneity in receptors, kinases, and other signaling components, critically shape the pathway dynamics. To capture these processes, we employed a compartmental modeling approach using ML-Rules, a multilevel rule-based language [49, 50]. Cellular and subcellular structures—such as the plasma membrane, raft domains, endosomes, and lysosomes—are represented as nested compartments with variable molecular content and attributes (e.g., radius, volume). ML-Rules enables the dynamic creation, merging, modification, and removal of compartments during runtime, allowing for a straightforward representation of processes such as endocytosis, recycling, and lysosomal degradation through declarative reaction rules [51]. Reaction kinetics may depend on compartment attributes, enabling volume-dependent rate kinetics and dynamic redistribution of molecular species. This approach provided us with the means to mechanistically incorporate the essential steps of the LRP6 receptor life cycle into a coherent, quantitative model.

To construct and calibrate the model, numerous experimental studies have been considered. Qualitative insights have been used to construct and structurally shape the model, while quantitative, time-dependent data were used for calibration and validation experiments, wherever available. The model was fitted concurrently to data regarding receptor complex dimerization, LRP6 phosphorylation, LRP6 internalization, and β-catenin aggregation. Integrating diverse experimental data from varying cell types, tissues, experimental conditions, and perturbations into a simulation model yielded comprehensive mechanistic insights into the role and impact of receptor trafficking.

Indeed, we find strong evidence suggesting a decisive role for receptor recycling in the short-term as well as long-term regulation of canonical Wnt signaling. Under the quantitative consideration of typical internalization rates of LRP6 and dimerization dynamics measured in vitro, we find that rapid recycling and sorting processes are required for the formation of large signalosomes. Furthermore, our results suggest that signalosome degradation and receptor recycling are crucial for maintaining stable, long-term Wnt signaling and sustaining β-catenin accumulation. This may explain why excessive pathway activation in cancer cells frequently depends on efficient internalization and recycling mechanisms, hence providing a promising, yet underestimated therapeutic target.

To summarize, our study highlights the complex interplay of cellular processes involved in Wnt signaling, including lateral diffusion, internalization, recycling, and the role of ordered membrane domains, and provides a foundation for identifying novel strategies to modulate Wnt pathway activity in disease contexts.

2 Results and Discussion

Here, we discuss aspects of receptor mobility and its impact on activation of the pathway, gained from our quantitative modeling. The mechanistic model of canonical Wnt signaling presented here was built using a bottom-up approach. Starting with a very simple model comprising a minimal set of reaction rules, we extended the model step-by-step by incorporating mechanisms reported in the literature. Our goal was to find a model for the initial steps in canonical Wnt signaling, i.e., Wnt binding, receptor aggregation, and signalosome formation, with parameter values within biologically reasonable limits that fit all of the following experimental data at the same time: 1) receptor dimerization (LRP6 and FZ) after Wnt binding, 2) LRP6 phosphorylation, 3) LRP6 internalization, 4) lipid rafts size distribution and 5) β-catenin aggregation.

Model

In the following, we describe the qualitative model that resulted from the progressive development of the model. Note that we discuss only the main molecular interactions, the major dynamics, and key assumptions to facilitate access and understanding of the model. Individual mechanisms are depicted in Figure 1. A detailed description of the modeling process, its underlying assumptions, and considerations can be found in the supplemental material.

Wnt receptor binding (A) The first step in the initiation of the signal transduction process is the binding of the ligand to its corresponding receptor. In the case of canonical Wnt signaling, signaling is initiated by the binding of specific Wnt proteins, such as Wnt3a or Wnt9, to membrane-associated LRP5/6 and Frizzled receptors. Numerous studies show that, under normal conditions, Wnt binding to both receptors, Frizzled and LRP6, is required to initiate canonical Wnt signaling [52, 53, 54]; and that binding to both receptors occurs simultaneously and independently [55]. Accordingly, the formation of the resulting trimeric ligand receptor complex (TRC) is modeled as a two-step process. First, extracellular Wnt binds to LRP6 or Fz. Subsequently, Wnt/FZ complexes bind to LRP6, or Wnt/LRP6 complexes bind to FZ. All processes are parameterized with the corresponding association and dissociation rate constants found in the literature [7, 52].

DVL binding (B) and receptor complex oligomerization (C) Importantly, recent findings suggest that a single trimeric receptor complex (TRC) does not suffice for pathway activation. Instead, activation requires the oligomerization of at least two trimeric receptor complexes, mediated by the cytoplasmic protein Dishevelled (DVL) [56, 55, 11]. Consequently, we include the recruitment of DVL to the membrane and its binding to TRC and assume that the experimentally determined rate of Dvl self-aggregation serves as an upper limit for the dimerization/oligomerization rate of receptor complexes bound to DVL [11, 54, 10]. In this step, we take into account the varying membrane dwell times

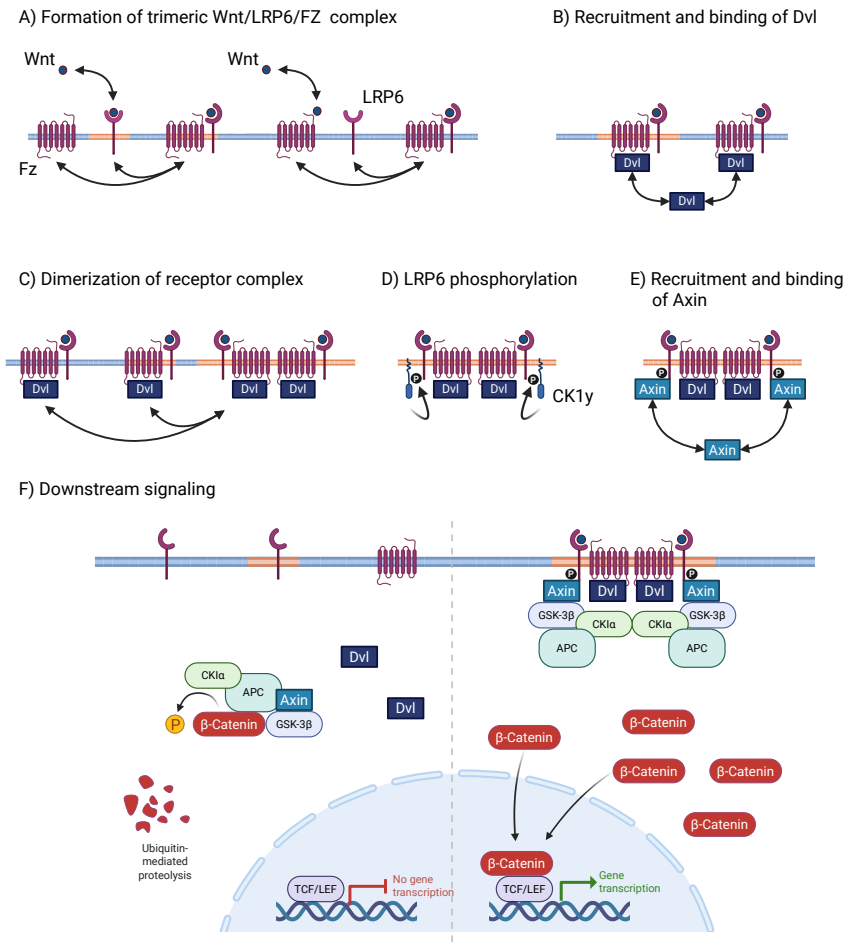

Figure 1: Simplified view of initial steps of signalosome formation and receptor activation after Wnt stimulus, as implemented in the model. The lower image (F) shows downstream signaling after successful signalosome formation in canonical Wnt signaling. The left side shows the inactive state (no Wnt stimulus), and the right side shows the activated state (with Wnt stimulus). Figure was

of DVL, which crucially depend on the localization of Frizzled [11] and the local membrane composition, in particular the PI(4,5)P2 concentration [57]. The exact implementation of DVL dwell times with respect to membrane composition will be described in the result section.

Receptor phosphorylation (D) and signalosome formation (E) DVL binding and receptor oligomerization prime the phosphorylation of multiple PPP(S/T)P motifs within the intracellular domain of membrane-anchored LRP6. In our model, we focus on the phosphorylation of site T1479 by membrane-associated CK1y, which is pivotal for subsequent signal transduction of canonical Wnt signaling [12, 13, 58, 59]. Phosphorylation of site T1490 within the membrane-proximal motif by membrane-associated GSK3β is more unspecific and primarily serves to prime the CK1-mediated phosphorylation of site T1479 [12, 16]. Importantly, this process is limited to cholesterol-rich liquid ordered (lipid raft) domains [13, 29, 60, 61]. Since only a minor fraction of LRP6 receptors are located in lipid rafts [29, 62, 31, 32], the membrane localization of the receptor complex represents one of the most rate-limiting properties in LRP6 phosphorylation and the activation of the receptor complex.

Receptor life cycle The dynamics of the receptor life cycle, including multi-complex formation, ligand- or raft-induced internalization, recycling, and intracellular sorting, present important yet challenging features to incorporate into a computational pathway model. Together with the resulting heterogeneous distribution of signaling components, such as receptors and kinases, these dynamics play a decisive role in canonical Wnt signaling. Here, we use a compartmental approach to represent cellular components (membrane or nucleus) and subcellular or membrane-based components (raft domains, endosomes, lysosomes) as individual entities. These entities may contain variable amounts of molecules (or other compartments) and may have arbitrary attribute values to represent important characteristics of the compartment, like its radius or volume. The model formalism used here, ML-Rules, enables the dynamic creation, modification, and removal of compartments during runtime [63, 64]. Processes like internalization, recycling, merging, or lysosomal degradation can be expressed straightforwardly in terms of reaction rules. Corresponding attributes, such as radius or volume, can be dynamically combined, modified, or newly specified. More importantly, these dynamic attributes are available for reaction rate calculations, allowing the specification of, e.g., individual volume-dependent reaction rate kinetics [51]. Species, such as molecules, located within a compartment, are handled according to the given rule, e.g., in the case of internalization, they are transferred from one compartment to the other, and in the case of compartmental degradation, all Based on this, we were able to incorporate most of the essential processes of the LRP6 life cycle during canonical Wnt signaling in our computational model, as depicted in Figure 2.

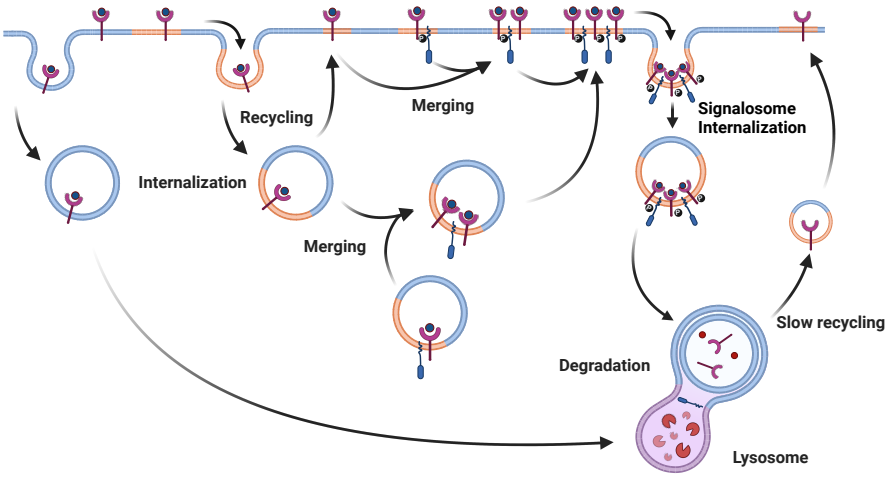

Figure 2: Simplified view of receptor life cycle as implemented in our model. Only LRP6 is considered, its binding state to FZ and cytosolic proteins, such as Dvl or Axin, are not shown. Created in BioRender. Haack, F. (2025) https://BioRender.com/nyn65rn

Downstream Signaling Once phosphorylated, the intracellular domain of LPR6 within the multimeric receptor complex (MRC) provides high-affinity binding sites for Axin. This induces the recruitment and binding of Axin and other components of the β-catenin destruction complex to the TRC at the membrane. This leads to the inhibition of the destruction complex and allows for β-catenin aggregation in the cytosol and nucleus. Reactions involving the LRP6 / axin interaction and subsequent downstream signaling events are part of a model that has previously been published and is being reused here [47].

Data-driven model building unravels three concurrent mechanisms driving receptor internalization in the initial phase of Wnt signaling

Important steps in the initial phase of canonical Wnt signaling are the formation of the trimeric receptor complex (i.e., the binding of the extracellular ligand Wnt to and the association of its cell surface receptors LRP6 and Frizzled) as well as its localization in ordered membrane domains. The binding kinetics between Wnt and its pathway-specific receptors LRP5/6 and Frizzled subtypes, as well as the molecular structure of the Wnt/Frizzled/LRP6 complex, have been well characterized [52, 7, 65]. However, the localization of the Wnt-receptor interaction, the impact of the membrane environment, and the role of posttranslational lipid modification of Wnt are still under discussion [66, 67]. Our quantitative, mechanistic modeling approach allows us to explore these processes in detail and provide quantitative evaluations of common theories, e.g., why Wnt is primarily located in ordered membrane domains, and what role palmitoylation of Wnt plays in this context.

While direct experimental observations under endogenous conditions are barely available, time-resolved experimental measurements on receptor dimerization [68, 69] and internalization (e.g. [29, 70, 71, 69]) provide valuable kinetic data. This data is used to evaluate different model scenarios with respect to the localization of Wnt and its binding to receptors FZ and LRP6. First, we consider LRP6 endocytosis induced by MESD, a specific ligand that binds LRP6 and induces its internalization. As MESD binds to LRP6 independently of its localization at the cell surface, kinetic rates for the internalization and recycling of LRP6 in response to unspecific MESD-LRP6 binding provide an upper bound for the internalization of LRP6 [70, 71]. The internalization of LRP6 in response to MESD treatment can be reproduced using a simple model comprising only three rules: MESD/LRP6 binding, LRP6 internalization, and LRP6 recycling.

Several studies report that, in contrast to MESD, Wnt binding to LRP6 selectively occurs in ordered membrane environments, where it gets internalized with the resulting receptor complex [61, 66, 67]. We performed several simulation experiments with different assumptions regarding the spatial restrictions of the Wnt-LRP6 interaction and the order of events leading to the formation of the trimeric receptor complex, consisting of Wnt-FZ-LRP6. For each assumption, we tried to fit the corresponding model to available experimental data on

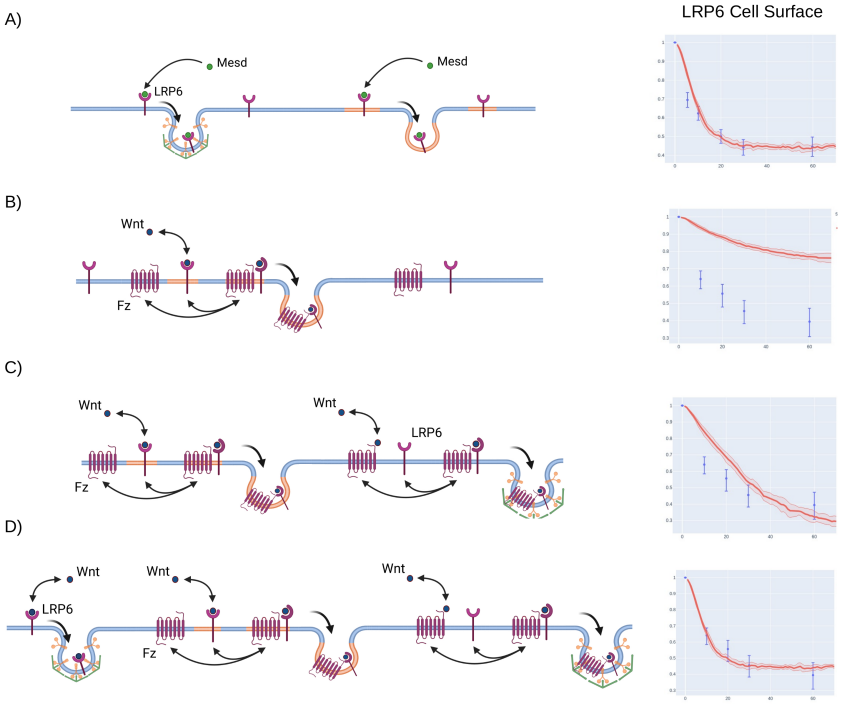

Figure 3: Comparing LRP6 internalization for different model scenarios. A) Simplified model representing MESD-induced internalization of LRP6. The trajectories exhibit a good fit to the experimental values measured in [71]. B) More complex model, in which Wnt binding is restricted to LRP6 in lipid raft domains. No binding occurs between Wnt and Frizzled. Apparently, the simulation result of the model with the best fit cannot reproduce the experimental data as measured, e.g., in [29]. C) Complex model, where Wnt binding to LRP6 is still restricted to raft domains, but FZ-Wnt interaction is allowed everywhere. D) Complex model, where Wnt binding to LRP6 and Frizzled is allowed everywhere. Created in BioRender. Haack, F. (2025) https://BioRender.com/7htzq6h

receptor dimerization and internalization. Intriguingly, our simulation results (Figure 3) indicate that Wnt binding to LRP6 in ordered domains alone does not quantitatively suffice to reproduce the internalization and receptor complex dimerization rates observed in vitro (e.g. [29, 69]). This can be explained as follows: with LRP6 being homogeneously distributed throughout the membrane, only a minor fraction (25-30 %) is located in ordered membrane environments [29, 60, 61, 66] and this distribution does not significantly increase after Wnt stimulation [29, 60]. Therefore, only a small fraction of LRP6 is available for Wnt binding and subsequent internalization, which is in contrast to most experimental measurements, indicating the internalization of large fractions of cell surface LRP6 (50-60%) within several minutes after Wnt stimulation [29, 72, 71].

Thus, according to our results (Figure 3), LRP6 internalization is orchestrated by three different mechanisms: FZ/Wnt/LRP6 complex internalization outside membrane domains, direct LRP6 internalization, and signalosome internalization in ordered membrane domains. Together, these concurrent processes yield the correct amount/fraction of internalized LRP6.

Still, the question remains: how to align our results with the observation that Wnt is selectively located in ordered membrane domains in vitro? A possible explanation is that, in contrast to most internalization assays that are performed directly after Wnt stimulation, the microscopy measurements in the corresponding experiments, e.g., by Sezgin et al., have been either conducted several hours after initial Wnt stimulation or using transfected cells expressing Wnt [66, 67]. This means these measurements were performed in the equilibrium state of the cells. Therefore, enough time has passed after Wnt binding such that receptor trafficking and protein sorting processes may steer the localization of Wnt-receptor complexes to raft domains.

Microdomains reinforce rebinding of DVL, which is crucial for the formation of multimeric receptor complexes

The localization of the Wnt/FZ/LRP6 complex (TRC) to ordered raft domains is extremely important for the stability of the receptor complexes, as shown in the next simulation experiments. Several studies indicate that the membrane affinity of DVL, and hence its membrane dwell time, highly depends on the membrane composition [31, 57, 32].

A model that incorporates the concept of rebinding (the process by which proteins return to their original location) and residence time (the duration a protein remains in a particular location) can explain how lipid rafts facilitate the recruitment and aggregation of proteins like DVL (Disheveled), which is crucial for Wnt signaling.

To illustrate this, we consider a small part of the entire model and use the resulting submodel for a set of simulation experiments. The simplified model contains a fixed number of established trimeric receptor complexes (TRC), which are either located in the membrane or in membrane sub-compartments representing ordered membrane domains, such as raft compartments, and an intracellular pool of DVL molecules that can associate with TRC. The residence time

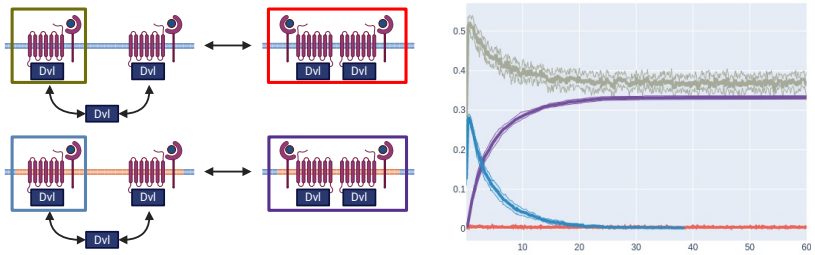

Figure 4: Simulation of sub-models containing a fixed number of trimeric receptor complexes (TRC), to which cytosolic DVL may bind or unbind. TRC with bound DVL form dimers. Colored boxes in the left figure correspond to the observed model entities, whose simulation trajectories are displayed on the right-hand side. Simulation trajectories indicate almost exclusive accumulation of DVL/TRC dimers in raft domains (purple) compared to non-raft regions (red). This due to the small volume of raft compartments and longer membrane residence time of DVL, facilitating immediate binding and rebinding of TRC located in the same raft compartment. Created in BioRender. Haack, F. (2025) https://BioRender.com/f5qyuaz

of DVL at the membrane, i.e., its dissociation rate from the receptor complex, depends on the localization of the TRC, as observed in several in-vitro studies [31, 11, 57]. As a result of the lower dissociation rate of the DVL-TRC complex in raft compartments, the equilibrium number of DVL bound to the receptor complexes in rafts is similar to the number of DVL-TRC complexes in the remaining membrane compartment - despite the fact that only 25% of RCs are located in raft compartments (red line vs brown line, preliminary Fig. 4). This effect is even stronger for the dimerization of the receptor complexes, mediated by DVL self-aggregation (purple vs blue line, preliminary Fig. 4), as only in raft compartments a stable population of DVL-TRC dimers is established. This is due to the low self-aggregation rate of DVL, which controls the dimerization of the TRC [10, 73, 59].

Due to the small volume of each individual raft compartment, the chance of immediate rebinding between DVL/TRC complexes before DVL disengages from the membrane is much higher than in the remaining (large) membrane compartment. This leads to a high (equilibrium) number of dimerized TRC in ordered membrane domains and a very low number of dimerized TRC in the remaining membrane. Thus, the simplified model provides an illustrative explanation of why aggregates of DVL and TRC are primarily located in ordered membrane domains and highlights the crucial role of these raft domains in recruiting and binding DVL to the receptor complex, leading to the formation of the signalosome.

Cross-compartmental mobility of membrane proteins is essentially required for the formation of large signalosomes due to sparse receptor density

After binding of pathway-specific Wnt proteins, the canonical Wnt signaling pathway requires the co-localization of LRP6 and Frizzled, subsequent receptor clustering, and signalosome formation to activate signal transduction. For this, the lateral mobility of membrane proteins is essentially required. Proteins and lipids undergo 2-dimensional lateral diffusion within fluid biological membranes. High-speed single-particle tracking revealed that membrane proteins diffuse freely only within ∼40–250 nm voxel bounded by actin "fences" [74]. For longer distances (and observation time), membrane-bound proteins yield a characteristic hop-diffusion behavior with effective diffusion coefficients being significantly lower compared to lateral diffusion rates within individual voxels [75, 76]. It is widely accepted that actin-associated scaffolds (for example, ERM proteins linking lipid rafts) can pre-cluster receptors by transiently co-anchoring them, and that the confinement through the cytoskeleton in general increases local receptor density and rebinding of ligand or effector molecules accelerating oligomerization (e.g., EGFR dimerization) and downstream signaling [75]. This presupposes that several pathway-specific membrane-anchored proteins or protein complexes are located in the same or in neighboring voxels. However, a quantitative consideration of the typical density of cell surface receptors compared to the size of voxels bound by actin "fences" reveals a surprisingly large separation of receptors: Assuming a mean cell surface of HeLa cell ($1,5x10^3\mu\mathrm{m}^2$) [77], the median size (length) of the cytoskeletal compartment in HeLa cells of 64nm [76], then an individual voxel covers $4096\mathrm{nm}^2$ or $4,096 \times 10^{-3}\mu m^2$. Projected to the entire cell surface, more than 360000 voxels span the cell surface. In contrast, typical numbers of cell surface receptors range between 1k and 10k. This means that, for homogeneously distributed receptors, there are not several receptors within one compartment; instead, single receptors must surpass tens or hundreds of actin "fences" to co-localize in the same compartment and interact. This issue potentiates as soon as the receptors form heteromeric receptor complexes. The density becomes even sparser, while confinement within a compartment increases with complex size, eventually leading to temporary immobilization within a membrane compartment. This is exactly the case in canonical Wnt signaling. Canonical Wnt signaling depends on the formation of a large receptor-protein complex, termed signalosome, initiated by co-localization of its pathway-specific receptors LRP6 and FZ after Wnt binding and subsequent recruitment of cytosolic proteins, such as DVL, Axin, and casein kinases. For successful receptor activation upon Wnt binding, Frizzled, LRP6, and Wnt need to form a trimeric receptor complex (TRC), followed by the recruitment and binding of cytosolic DVL (D-TRC). Recent studies indicate that at least two of these receptor protein complexes are needed for a multimeric receptor complex (MRC) [55, 65]. The aggregation of the multimeric receptor itself and its fusion with other MRCs to form larger signalosomes is supposed to be driven by lateral diffusion [13, 55, 78].

Signalosome formation is promoted by intracellular shuttling

Experimental measurements show that receptor cluster size in canonical Wnt signaling can reach up to ∼100 nm [79]. As outlined before, larger protein complexes are located in distinct membrane compartments surrounded by an actin skeleton and protein "picket" fences, hence mostly immobilized when crossing a certain threshold size (>20 nm) [80, 79, 81]. In canonical Wnt signaling, this upper threshold roughly applies to dimerized TRC and any larger receptor complex, hence all species we consider as MRC. Considering the complex mechanisms and large receptor protein complexes required to activate signal transduction in canonical Wnt signaling, we examine whether signalosome formation is achievable just by passive lateral diffusion or whether active mechanisms are additionally required to support receptor aggregation and signalosome formation.

To analyze the impact of immobilization of multimeric receptor complexes (MRC) on the formation of signalosomes, we consider model scenarios in which single TRC are always mobile, while higher-order receptor complexes (MRC) are immobile for varying Wnt stimuli. Here, larger receptor complexes emerge only by the lateral association of TRC with existing MRC. Fig. (5) shows the number of TRC molecules located in dimers, medium-sized (<100 nm, or large MRC (>100 nm) for low, medium, or high Wnt stimuli. Surprisingly, given that MRC are mostly static and form immobile clusters, as suggested by the literature (e.g. [82, 79]), we find that only a small amount of medium-sized and no large receptor clusters form, even for high Wnt stimuli (see Fig. 5). For many years, numerous studies have suggested a beneficial role of receptor trafficking in various signaling pathways [33, 83, 84]. Endosomal compartments may concentrate ligands and downstream adaptors, which prolongs kinase activity (e.g., EGFR, β-adrenergic receptors), while endosomal transport can induce receptor sorting, based on distinct lipid environments [37, 35].

Although numerous studies over the last 20 years have shown the important role of internalization in Wnt signaling, and our simulation experiments have confirmed this, few studies exist that have actually analyzed the potential role of receptor trafficking and recycling in Wnt signaling [14, 85]. Cholozza et al. revealed rapid recruitment of endosomal/ESCRT components to LRP6 using time-resolved proximity labeling after Wnt stimulation, establishing a mechanistic link between endosomal receptor trafficking and Wnt signal propagation [40].

We therefore ask whether receptor trafficking, endosomal sorting, and recycling might also play a beneficial role in Wnt signaling, as recently discussed for other signaling pathways, and include these processes in our model.

Note that we differentiate between raft-associated and non-raft-associated internalization: Endocytosis of receptor or receptor complexes bound to Wnt outside of raft domains is most likely mediated by ZNRF3 and RNF43, leading to degradation of the receptor complex and slow recycling [18]; whereas endocytosis of raft-associated receptor or receptor complexes bound to Wnt is subject to

intracellular transport, hence quickly recycled back to the membrane, where they merge with existing raft domains [86, 87, 88]. Receptor complexes that are phosphorylated and in complex with members of the destruction complex (in our model simply represented by AXIN species), hence fully assembled signalosomes, are transferred to the lysosomal degradation pathway upon internalization.

Intriguingly, including receptor trafficking mechanisms in our model results in numerous medium-sized and even large signalosomes, as observed in vitro [13, 79, 89, 78] (Fig. 7).

This result can be explained as follows: Once internalized, we can assume that the mobility of receptor-bearing endosomes is higher than lateral mobility at the membrane. Note that this aspect becomes even more relevant considering our quantitative analysis of receptor density and compartmentalization of the membrane (see above). While lateral diffusion of the receptor complexes is likely subject to local immobilization and hop diffusion, receptor-bearing endosomes might further be subject to active, intracellular transport, which potentially further increases the mobility of receptor complexes located in early endosomes. In addition, active sorting has been observed for endosomes with high content of saturated lipids and cholesterol; studies show a gradient of lipid composition, which shifts from saturated to unsaturated lipids with increasing distance from the cell surface [90]. This means, in contrast to pure lateral association of TRCs and MRCs, the internalization and recycling support and enhance the localization of receptor complex components, such as LRP6, Frizzled, and Dvl, in microdomains that are enriched in cholesterol and saturated lipids [88].

In summary, to arrive at the size of large receptor clusters as described in the literature, an active sorting mechanism is required, most likely mediated, or at least supported, through internalization.

To better understand this simulation result, we analyze the firing rate of each individual rule defined in our simulation model throughout the simulation runs. In Figure 6, the main processes with respect to receptor trafficking implemented in our model are illustrated with arrow color (gray and red) refering to the simulation models and arrow width being scaled with the mean firing rate of the corresponding rule in our simulation model. Here, it becomes obvious that in a model without receptor trafficking (gray arows) the majority of TRC and small MRC are internalized before they can merge with each other. This limits the aggregation of TRC into larger MRC clusters, hence limits the size of MRC. Visualizing the rule count distribution of the model with receptor trafficking (red arrows) reveals a more even distribution of rule firing rates, indicating a more balanced and fine-tuned activation of various, concurrent mechanisms. Lateral association of TRC (dimerization) as well as intracellular transport (i.e., recycling of early endosomes) contribute to and promote the assembly of stable signalosomes. On the other hand, the intensity of the signal activation is limited and controlled by caveolin-mediated degradation of signalosomes as well as early ZNRF3 and RNF43 induced internalization and degradation of TRC (Fig. 6).

Lastly, fast receptor trafficking might also explain the primary localization of Wnt proteins in raft domains several hours after Wnt stimulation or in trans-

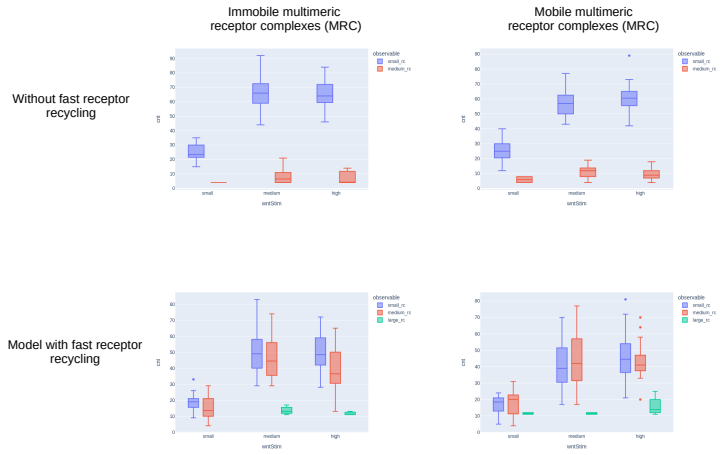

Figure 5: Distribution of small (blue), medium (red) and large (green) receptor complexes in varying model scenarios. In a model including internalization and fast recycling the amount of medium and large receptor complexes is largely increased, indicating that these processes are required for the formation of large signalosomes.

fected, Wnt-producing cells, as observed in [66]. While Wnt-receptor complexes outside of raft domains are quickly internalized and degraded, raft-specific recycling and protein sorting steer the localization and enrichment of Wnt-receptor complexes to raft domains. This process results in the predominant localization of Wnt proteins to raft domains.

Lack of fast recycling attenuates LRP6 dimerization and phosphorylation leading to significantly reduced β-catenin accumulation.

Our simulation results reveal a promoting effect of receptor trafficking on receptor clustering and signalosome formation. In the literature, increased receptor clustering and larger signalosomes typically imply an improved receptor activation as well as higher downstream signal output. To check whether this also applies to our model, we analyze the impact of receptor trafficking on LRP6 phosphorylation, and eventually on signal transduction in terms of β-catenin aggregation. Figure 7 shows the mean trajectories of model simulation with and without receptor trafficking under medium Wnt stimulus.

As expected, the higher amount of larger signalosomes obtained in the model

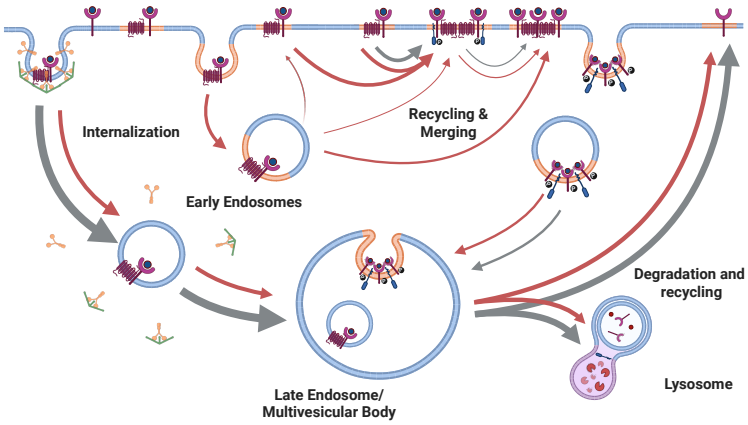

Figure 6: Comparison of rule counts of models with (red arrows) and without (gray arrows) intracellular receptor traffic. Arrow width scales with rules fired in simulations of the corresponding model (indicated by arrow color). Created in BioRender. Haack, F. (2025) https://BioRender.com/dymsp27

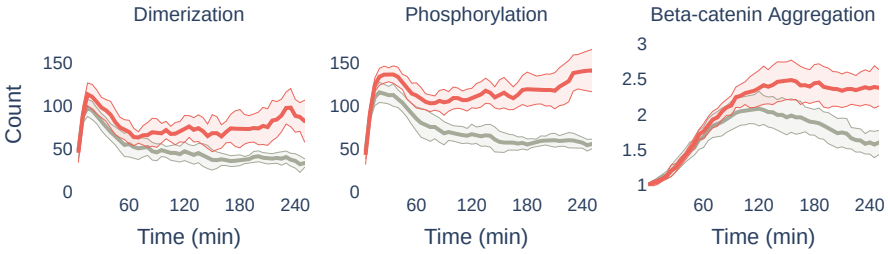

Figure 7: Mean simulation trajectories for receptor dimerization (left), phosphorylation (middle) and nuclear β-catenin concentration (right, fold change). The red line corresponds to simulation trajectories of a model with receptor trafficking and fast recycling. The grey line shows simulation trajectories of a model missing fast receptor recycling. Simulation results suggest, that the lack of fast recycling attenuates TRC dimerization and phosphorylation, leading to reduced β-catenin signaling.

with receptor trafficking also yields a higher amount of phosphorylated LRP6 receptors as well as β-catenin counts in the nucleus. This indicates an attenuated pathway activity in a model lacking intracellular receptor trafficking. Interestingly, the deviation between the two scenarios (receptor trafficking vs. pure lateral diffusion) is small in the very early response after the onset of Wnt stimulation, but strongly increases after several minutes. The reason for this is that dimerization of TRC is sufficient for LRP6 phosphorylation and downstream signaling, a process achieved and primarily controlled by lateral diffusion directly after the onset of Wnt stimulation [91, 11]. However, TRC and dimerized receptor complexes are both subject to internalization. In the model scenario without fast recycling (gray color in Figure 7) all receptor complex entities are primed for degradation and slow recycling. In contrast, in a model with fast recycling raft-associated receptor complexes (mono and dimers of TRC) are recycled back to the membrane within several minutes, yielding larger and more stable signalosomes, that amplify LRP6 phosphorylation, and β-catenin stabilization, hence downstream signaling. This is in line with the general time frame typically obtained for fast recycling processes, which are in the range of $\sim$ 3-5 minutes [37, 92, 93].

Sustained, long-term Wnt signaling depends on internalization and receptor recycling

Notably, comparing model scenarios with and without receptor trafficking revealed that the effect of receptor trafficking not only transiently promotes the signal transduction, but also leads to a more sustained, long-term stabilization of β-catenin levels. Sustained, long-term activation of the Wnt/β-catenin pathway is mandatory for numerous physiological processes, such as embryonal patterning and morphogenesis (e.g. [94]), adult stem-cell maintenance and self-renewal (especially in intestinal crypts) (e.g. [4, 1]), and tissue regeneration (e.g. [3]). At the same time sustained, long-term Wnt/β-catenin is an important hallmark of Wnt-induced cancer [95].

To analyze the impact of receptor trafficking on long-term Wnt signaling and for a more detailed model exploration, we employ a recent visual analytics approach [96]. In this visualization design, time series plots are embedded in parallel coordinates, enabling a simultaneous and interactive visual analysis of numerical model parameters and simulated signaling behaviors over time.

In the visualization, each line in the graph corresponds to an individual model configuration that has been simulated in the course of a parameter scan (see Figures (8 and 9). The gray parallel axes depict the individual parameter values employed in the parameter scan (e.g., kRaftInternalization, kRaftRecycling, kRaftDegradation), whereas the colored axes depict simulation trajectories of a certain model observable, such as LRP6 internalization (LRP6Int) or nuclear β-catenin levels clustered into groups of similar time series.

The visualization allows for exploring the relation between certain model configurations and model outputs in more detail. For instance, Figure 8 shows two noteworthy model configurations, highlighted in orange and blue, where the

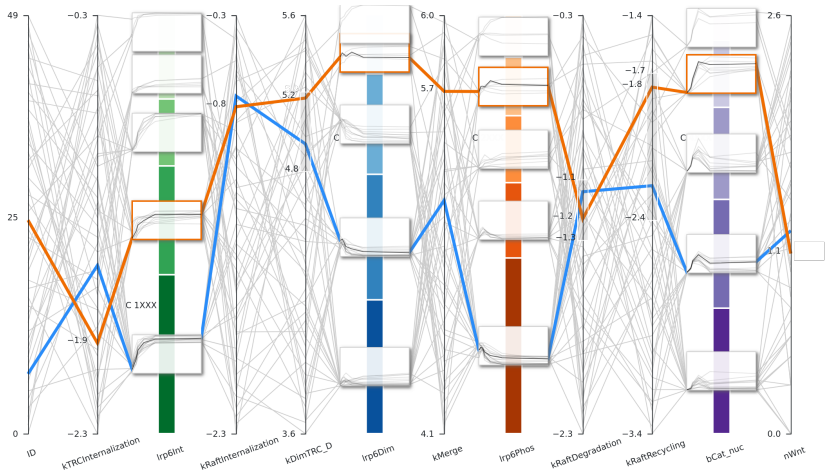

Figure 8: Parallel coordinates depicting parameter values of various model configurations (lines) and corresponding simulation results (boxes of clustered trajectories). Two model configurations highlighted in the figure by orange and blue lines illustrate the impact of varying the parameter values for fast and slow recycling (kMerge, kRaftRecycling) on output variables, such as phosphorylation in red, LRP6dimerization blue, and in particular on β-catenin aggregation (shown in purple).

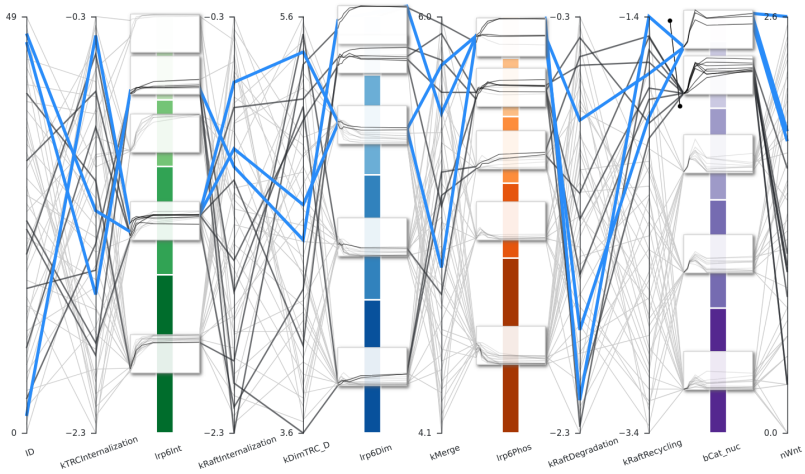

Figure 9: Parallel coordinates depicting parameter values of various model configurations (lines) and corresponding simulation results (boxes of clustered trajectories). In the figure all model configurations are highlighted, that lead to high and stable β-catenin aggregation, for high and medium Wnt stimulus.

simulation trajectories show very different model outcomes in terms of LRP6 dimerization (blue axis), phosphorylation (red/orange axis), and β-catenin accumulation (violet axis), despite similar parametrization and Wnt stimulus (nWnt). The only parameter values that differ significantly between the model configurations are related to fast and long-term recycling (kMerge and kRaftRecycling), which supports our previous observation that receptor trafficking has an unexpectedly strong impact on β-catenin aggregation.

Next, we ask which parameter value combinations are required for the optimal – i.e., strongest – activation of the pathway. For this, we consider all simulation trajectories with the highest and most stable β-catenin accumulation. These trajectories are displayed in the uppermost group of the β-catenin axis in Figure 9. By selecting this group we highlight all model configurations that yield the corresponding simulation trajectories (blue lines).Intriguingly, model configurations that result in the most efficient signaling outcome have a clear pattern and are characterized by high values of slow receptor recycling (kRaftRecycling) and moderately high values of parameters associated with receptor internalization and fast recycling (kRaftInternalization, kMerge). Extending the selection to the second group of high, stable β-catenin (black lines, Fig. 9) results in a more diverse parameter value distribution, which means that not every parameter value of receptor recycling has to be high. The only exception is the parameter value of slow receptor recycling (kRaftRecycling) and to some extent fast receptor recycling (kMerge), which are essentially required to be high for long-term β-catenin stabilization.

To challenge our previous insights drawn from the visualization and to quantify how changes in the regulation of membrane dynamics alter the signal outcome hours after signal initiation, we apply a global sensitivity analysis using the Sobol' method. We specifically vary the parameter values of all processes related to receptor trafficking and observe β-catenin accumulation in the nucleus at different time points after signal initiation (30 minutes, 1 hour, 6 hours, and 12 hours).

As a result of the sensitivity analysis, we observe a surprisingly strong difference in Sobol indices between early, transient (30 minutes and 1 h) and late, long-term response (6h and 12h). For early time points, the kinetic rate for trimeric receptor complex dimerization driven by lateral diffusion (kDimTRC_D) has the highest Sobol indices (global (ST) as well as first-order (S1)), followed by parameters related to receptor trafficking (kRaftInternalization, kRaftRecycling, kRaftDegradation). This is in line with our previous results. For later time points, however, the recycling rate (kRaftRecycling) of internalized and degraded receptor complexes is the dominating parameter that controls β-catenin levels. These results imply that different mechanisms control β-catenin stability, hence pathway activity, in a time-dependent manner and that recycling plays a surprisingly vital role in long-term β-catenin signaling.

To explain these results, we need to consider the signaling logic of canonical Wnt signaling, which is fundamentally distinct from other prominent signaling pathways, such as EGFR or TGF-β. Instead of inducing the intracellular signal transduction by G-proteins or kinase cascades, canonical Wnt signaling is regu-

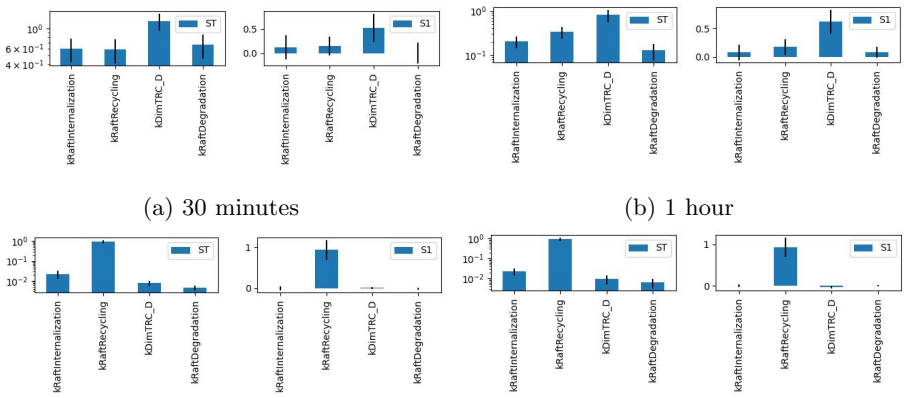

(a) 30 minutes (b) 1 hour

(c) 6 hours (d) 12 hours

Figure 10: Global (ST) and first-order (S1) Sobol indices indicating model sensitivity (in terms of beta-catenin concentration) against changes in receptor trafficking dynamics measured at different time points after onset of WNT stimulation. Parameters with high Sobol indices differ between early, transient (30 minutes and 1 h) and late, long-term response (6h and 12h) indicating

lated post-translationally by stabilizing the pathway's target protein β-catenin. This is achieved by the recruitment and binding of essential components of the destruction complex, which limits β-catenin levels by continuous degradation, to the multimeric receptor complex (MRC) that forms upon binding of Wnt to its co-receptors Frizzled and LRP5/6 and subsequent receptor clustering (as described in previous sections). Since the signalosome lacks downstream enzymatic amplification steps, signal persistence depends solely on ongoing ligand-receptor clustering and the inhibition of β-catenin degradation, rather than second-messenger kinetics.

Here, the scaffold proteins AXIN/AXIN2 play a crucial role. AXIN is the rate-limiting scaffold of the β-catenin destruction complex because it is present at very low cellular concentrations and serves as the central platform that recruits all other key components (APC, GSK3, CK1) [97, 98]. Upon Wnt activation, AXIN is rapidly recruited to LRP5/6 and is co-internalized with the receptor complex into caveolin-enriched endocytic vesicles / multivesicular bodies (MVBs), where destruction-complex components (AXIN, GSK3) become sequestered. Since AXIN availability dictates destruction complex formation, its depletion quickly induces β-catenin accumulation [97, 99]. However, the axin-related protein AXIN2 (also called Conductin) is a well-established transcriptional target of β-catenin/TCF complexes and is induced by active Wnt signaling [15, 100, 4]. Both AXIN proteins are functionally equivalent in vivo [101]. In contrast to AXIN1, which is constitutively expressed, AXIN2 expression increases following pathway activation and acts as part of a delayed negative feedback loop in canonical Wnt signaling [102, 103, 104].

Accordingly, the degradation of endogenous AXIN, induced by LRP5/6, has been considered to be a critical event in canonical Wnt signaling from early on [105, 106, 107] However, in view of our findings revealed by quantitative modeling, one important aspect has been neglected: If internalization and subsequent lysosomal degradation of the entire signalosome are the driving mechanisms for AXIN degradation, the recycling of LRP6 is essential to achieve a continuous receptor engagement of AXIN. Without a continuous round of receptor recycling, long-term Wnt signaling either leads to the depletion of cell surface LRP6 receptors, which lowers receptor density and signal activation efficiency (see above), or eventually all LRP6 receptors at the cell surface will be engaged in signalosomes, limiting the availability for newly synthesized AXIN2 proteins.

From a quantitative perspective, none of the known feedback mechanisms is capable of compensating for the negative feedback loop of AXIN/AXIN2, which is required for sustained, long-term Wnt signaling. While AXIN2 expression increases after pathway activation, the resulting protein does not uniformly restore β-catenin degradation because its stability and function are themselves regulated by Wnt-dependent post-translational mechanisms, including tankyrase-mediated turnover [108] However, tankyrase expression is generally not transcriptionally co-regulated with β-catenin–driven AXIN2 expression, and neither shows a reliable correlation across tissues or experimental conditions. Moreover, AXIN2 participates not only in the cytoplasmic destruction complex but also contributes to the assembly of the membrane-proximal signalosome, thereby conferring context-dependent roles in both attenuating and facilitating Wnt pathway output [109, 104, 110].

Lastly, there is no experimental evidence that LRP6 expression is correlated with canonical Wnt activation; on the contrary, several studies report a negative-feedback regulating β-catenin through LRP6 desensitization and downregulation of LRP6 expression [72, 71].

3 Conclusion

In our simulation model, we combined a multitude of experimental observations into a coherent explanatory framework that also considers the quantitative properties and dynamics of the system. For this purpose, a newly optimized multi-level rule-based modeling and simulation approach is employed to describe and simulate the compartmental distribution of extracellular, intracellular, and membrane-associated signaling molecules, as well as provide a concise representation of the receptor life cycle, including internalization, degradation, and recycling processes.

The results of our modeling and simulation study reveal that canonical Wnt signaling is not characterized by one, but rather several internalization mechanisms, which all play varying yet pivotal roles in early, mid-term, and long-term regulation. Our results suggest a previously underestimated role of receptor trafficking and recycling, particularly during mid- and long-term regulation. The observation that receptor distribution, in general, is much sparser than

the membrane compartmentalization by actin-cytoskeleton implies that receptor complexes have to overcome several membrane fences to co-localize. Therefore, effective receptor clustering relies on directed trafficking via internalization and fast recycling particularly to form larger protein complexes, as suggested by our simulation results.

Once established, large signalosomes are eventually internalized, and important components of the destruction complex, which have been recruited to the membrane, are sequestered in multivesicular bodies and eventually primed for lysosomal degradation. However, without continuous rounds of receptor recycling, long-term Wnt signaling leads to the depletion of cell surface LRP6 receptors, which lowers receptor density and signal activation efficiency.

Our model analysis reveals that high raft-associated internalization and elevated recycling lead to prolonged β-catenin signaling, while lowering internalization and recycling dynamics reduces pathway activation in terms of β-catenin aggregation more effectively than reducing the Wnt stimulus. This becomes particularly relevant in certain APC-mutant cancer cells, as recent studies uncovered that Wnt-independent formation of LRP6 signalosomes in APC-deficient cancer cells requires clathrin-mediated endocytosis and recycling. Further, the membrane composition, particularly in terms of cholesterol and fatty acid (omega-3 and omega-6) content, significantly impacts signalosome formation and internalization. Elevated levels of cholesterol and raft domains have been described as a hallmark of many cancer types. Controlling internalization and regulating receptor trafficking might thus provide a promising approach to handle excessive Wnt pathway activation in disease contexts, such as cancer.

Materials and Methods

Methods and Algorithms

To develop the model, a modeling approach is required that supports dynamic compartmentalization, including the creation of new compartments, their deletion, and merging.

Rule-based modeling based on ML-Rules Incorporating compartmental dynamics poses significant challenges for both the design of modeling languages and the underlying simulation engines. Many simulation tools in cell biology offer static compartments that do not change. This allows the modeler to consider the causal influence of compartments on the processes within. However, to account for the causal influence of the occurring processes on the compartmental structure and interactions, dynamic compartments are needed. ML-Rules is a rule-based language for multi-level cell biological modeling and supports a wide range of compartmental dynamics [49]. Various simulators have been developed for ML-Rules over the last decade [50]. Here, we use a more recent ML-Rules implementation in Rust that offers the required efficiency to model 1000s of compartments [51].

Model parameter calibration and validation The parameter values for our model were reused from previously published sub-models, particularly regarding intracellular downstream signaling, which were extracted from the literature or calculated based on experimental measurements. The remaining parameter values for which experimental measurements or literature were unavailable were fitted against various sources of experimental data using a genetic optimization algorithm that iteratively refined candidate parameter sets to reproduce data from in-vitro measurements. Starting off with a vector of initial candidate parameter values, i.e., the initial population, the simulation model was executed and its output was evaluated using a composite objective function. Note that our objective function consisted of multiple equally weighted distance metrics, each quantifying the deviation between simulated results and distinct experimental observations. This approach allowed us to simultaneously fit our model against various time-resolved in-vitro measurements on dimerization of trimeric receptor complex [91], LRP6 phosphorylation [69, 111, 112], and LRP6 internalization [29, 72, 71]. These metrics, i.e., the root mean square deviation of each model observable from the corresponding experimental data, were averaged across the available time points, normalized, and transformed into a fitness score that was used in the selection process of the population. Across successive generations, individuals with higher fitness were preferentially selected for crossover and mutation, generating new candidate solutions while maintaining population diversity. This evolutionary process continued until the convergence criteria (simulation trajectory of each observable lies within the measurement error bounds for all time points) were reached, at which point the best-performing parameter vector was identified as the calibrated model configuration.

After successfully calibrating the model parameter values, we conducted a cross-validation experiment by mimicking the in-vitro experiments performed in [113]. We initialized our model with the same range of Wnt concentrations as applied in [113] and measured the accumulation of intracellular (total) β-catenin 2 hours after the start of the stimulation. As depicted in Figure 11, the response curve is in good agreement for all Wnt3a concentrations applied. Thus, our model, which has been fitted against experimental data retrieved from various experimental sources, is also capable of reproducing β-catenin kinetics reported for different Wnt3a stimuli. Major insights drawn from the model-building and calibration process, as well as subsequent simulation experiments, will be discussed in the following.

Data

In the following model parameters for which experimental measurements exist are listed. Parameter values belonging to previously published model components reference the original data source, and, in case of calibrated values, to the publication where the model parameter has been fitted.

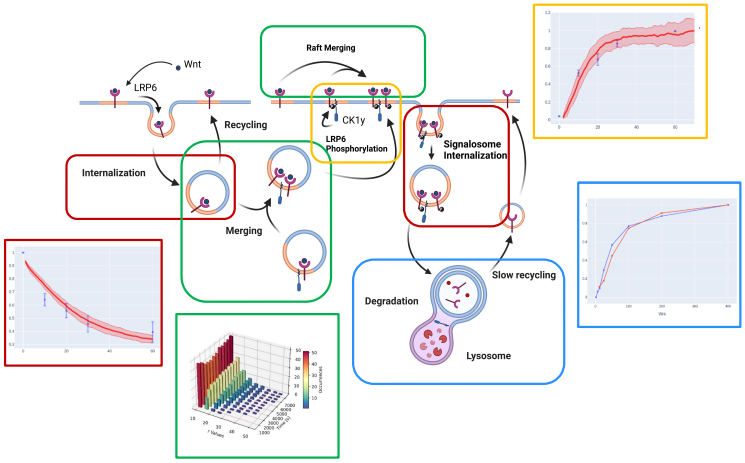

Figure 11: Model elements fitted against experimental data from various sources, including LRP6 phosphorylation (yellow), receptor dimerization and signalosome formation (green) and LRP6 internalization. In-vitro data of β-catenin aggregation obtained 2 hours after onset of Wnt stimulus for varying Wnt concentrations was used to validate the calibrated model. In the individual graphs, red lines correspond to simulation trajectories, whereas blue points represent experimental measurements. Created in BioRender. Haack, F. (2025) https://BioRender.com/cwdveej

Parameter	Name	**Description**	**Value**	**Reference**
k1	kLWntBind	Association rate constant between Wnt3a and LRP6	$3.62 \cdot 10^4\,\mathrm{M}^{-1}\,\mathrm{s}^{-1}$	[52]
k2	kLWntUnbind	Dissociation rate constant between Wnt3a and LRP6	$3.31 \cdot 10^{-4}\,\mathrm{s}^{-1}$	[52]
k3	kFWntBind	Wnt3a-Fz binding	$2.9 \cdot 10^4\,\mathrm{M}^{-1}\,\mathrm{s}^{-1}$	[52, 53]
k4	kFWntUnbind	Wnt3a-Fz unbinding	$1.4 \cdot 10^{-4}\,\mathrm{s}^{-1}$	[52, 53]
k5	kLF_bind	Formation of Trimeric receptor complex (TRC)	$4.82 \cdot 10^3\,\mathrm{nm}^2\,\mathrm{s}^{-1}$	[52, 53]
k6	kTRC_unbind	Dissociation of trimeric receptor complex (LRP6 from RC)	$2 \cdot 10^{-2}\,\mathrm{s}^{-1}$	[52, 31, 53]
k7	kDvlOn	DVL association to TRC	$5 \cdot 10^5\,\mathrm{M}^{-1}\,\mathrm{s}^{-1}$	[31, 11]
k8	kDvlOff_m	DVL membrane dissociation (membrane)	$4 \cdot 10^{-2}\,\mathrm{s}^{-1}$	[31, 11]
k9	kDvlOff_r	DVL membrane dissociation (raft)	$7.5 \cdot 10^{-3}\,\mathrm{s}^{-1}$	[31, 11]
k10	kDimTRC_D	Upper Bound for association of TRC (Dimerization)	$4 \cdot 10^4\,\mathrm{dm}^3\,\mathrm{M}^{-1}\,\mathrm{s}^{-1}$	[114, 11]
k11	kDimMRC_D	Upper bound for MRC association	$0\,\mathrm{M}^{-1}\,\mathrm{s}^{-1}$	[54, 11]
k12	kDimTRC_unbind	Unbinding frequency for TRC	$1.96 \cdot 10^{-1}\,\mathrm{s}^{-1}$	[54, 11]
k13	kMerge	Intracellular transport	$1.85 \cdot 10^5\,\mathrm{nm}^2\,\mathrm{s}^{-1}$	*
k14	k_gpiMerge	Mobility of GPI-anchored proteins	$8.18 \cdot 10^5\,\mathrm{nm}^2\,\mathrm{s}^{-1}$	—
k15	kLrpEndo	LRP6 internalization rate	$1.5 \cdot 10^{-1}\,\mathrm{min}^{-1}$	[37]
k16	kLrpRec	LRP6 recycling rate	$3.84 \cdot 10^{-2}\,\mathrm{min}^{-1}$	*
k17	kRaftInternalization	Raft internalization rate	$1.54 \cdot 10^{-1}\,\mathrm{min}^{-1}$	[37]
k18	kTRCInternalization	TRC internalization rate	$2.16 \cdot 10^{-1}\,\mathrm{min}^{-1}$	[37]*
k19	kTRCDegradation	TRC degradation rate	$3.89 \cdot 10^{-2}\,\mathrm{min}^{-1}$	*
k20	kRaftRecycling	Raft recycling rate	$1.76 \cdot 10^{-2}\,\mathrm{min}^{-1}$	*
k21	kRaftDegradation	Raft degradation rate	$7.5 \cdot 10^{-2}\,\mathrm{min}^{-1}$	*
k22	kLp	LRP6 phosphorylation rate	$2.412 \cdot 10^3\,\mathrm{M}^{-1}\,\mathrm{min}$	[47]
k23	kLdp	LRP6 de-phosphorylation rate	$4.7 \cdot 10^{-2}\,\mathrm{min}$	[47]
k24	kLAxinBind	LRP6-Axin association rate	$5 \cdot 10^5\,\mathrm{M}^{-1}\,\mathrm{s}^{-1}$	[31, 47]
k25	kLAxinUnbind	LRP6-Axin dissociation rate	$1.8 \cdot 10^{-4}\,\mathrm{s}^{-1}$	[31, 47]
k28	kAAp	Axin activation (phosphorylation) rate	$3 \cdot 10^{-2}\,\mathrm{min}^{-1}$	[97, 115, 47]
k29	kApA	Axin de-activation (dephosphorylation) rate	$3 \cdot 10^{-2}\,\mathrm{min}^{-1}$	[97, 115, 47]
k30	kAdeg	Axin degradation rate	$4.48 \cdot 10^{-3}\,\mathrm{min}^{-1}$	[97, 115, 47]
k31	kAsyn	Axin synthesis rate	$7.6 \cdot 10^{-10}\,\mathrm{M}\,\mathrm{min}^{-1}$	[97, 115, 47]
k32	kBetaSyn	β-catenin synthesis rate	$1.14 \cdot 10^{-3}\,\mathrm{M}\,\mathrm{min}^{-1}$	[97, 115, 47]
k33	kBetaDegAct	Active β-catenin degradation	$1.1 \cdot 10^2\,\mathrm{M}^{-1}\,\mathrm{min}^{-1}$	[97, 115, 47]
k34	kBetaDeg	β-catenin degradation rate	$1.13 \cdot 10^{-4}\,\mathrm{min}^{-1}$	[97, 115, 47]
k35	kBetaIn	β-catenin import rate	$2.886 \cdot 10^5\,\mathrm{M}^{-1}\,\mathrm{min}^{-1}$	[97, 115, 47]
k36	kBetaOut	β-catenin export rate	$2.886 \cdot 10^5\,\mathrm{M}^{-1}\,\mathrm{min}^{-1}$	[97, 115, 47]

Funding

The author(s) declare that financial support was received for the research and/or publication of this article. This work is in part supported by the German Research Foundation (DFG) within the Collaborative Research Center (SFB) 1270/2 ELAINE 299150580.

Generative AI statement

The author(s) declare that no Gen AI was used in the creation of this manuscript.

References

[1] Maxime Gasnier, Hui Yi Grace Lim, and Nick Barker. Role of Wnt signaling in the maintenance and regeneration of the intestinal epithelium. *Current Topics in Developmental Biology*, 153:281–326, 2023.

[2] Yiwei Li, Maorong Chen, Jiliang Hu, Ren Sheng, Qirong Lin, Xi He, and Ming Guo. Volumetric Compression Induces Intracellular Crowding to Control Intestinal Organoid Growth via Wnt/β-Catenin Signaling. *Cell Stem Cell*, 28(1):63–78.e7, January 2021.

[3] Zachary Steinhart and Stephane Angers. Wnt signaling in development and tissue homeostasis. *Development (Cambridge, England)*, 145(11):dev146589, June 2018.

[4] Hans Clevers and Roel Nusse. Wnt/β-Catenin Signaling and Disease. *Cell*, 149(6):1192–1205, June 2012.

[5] Chen Xue, Qingfei Chu, Qingmiao Shi, Yifan Zeng, Juan Lu, and Lanjuan Li. Wnt signaling pathways in biology and disease: Mechanisms and therapeutic advances. *Signal Transduction and Targeted Therapy*, 10(1):106, April 2025.

[6] Ken M. Cadigan and Mark Peifer. Wnt Signaling from Development to Disease: Insights from Model Systems. *Cold Spring Harbor Perspectives in Biology*, 1(2):a002881, August 2009.

[7] Stephane Angers and Randall T. Moon. Proximal events in Wnt signal transduction. *Nature Reviews Molecular Cell Biology*, June 2009.

[8] Christof Niehrs. The complex world of WNT receptor signalling. *Nature Reviews Molecular Cell Biology*, 13(12):767–779, December 2012.

[9] Ellen Youngsoo Rim, Hans Clevers, and Roel Nusse. The Wnt Pathway: From Signaling Mechanisms to Synthetic Modulators. *Annual Review of Biochemistry*, 91(1):571–598, 2022.

[10] Thomas Schwarz-Romond, Marc Fiedler, Naoki Shibata, P. Jonathan G. Butler, Akira Kikuchi, Yoshiki Higuchi, and Mariann Bienz. The DIX domain of Dishevelled confers Wnt signaling by dynamic polymerization. *Nature Structural & Molecular Biology*, 14(6):484–492, June 2007.

[11] Wenzhe Ma, Maorong Chen, Hong Kang, Zachary Steinhart, Stephane Angers, Xi He, and Marc W. Kirschner. Single-molecule dynamics of Dishevelled at the plasma membrane and Wnt pathway activation. *Proceedings of the National Academy of Sciences*, 117(28):16690–16701, July 2020.

[12] Gary Davidson, Wei Wu, Jinlong Shen, Josipa Bilic, Ursula Fenger, Peter Stannek, Andrei Glinka, and Christof Niehrs. Casein kinase 1 γ couples Wnt receptor activation to cytoplasmic signal transduction. *Nature*, 438(7069):867–872, December 2005.

[13] Josipa Bilic, Ya-Lin Huang, Gary Davidson, Timo Zimmermann, Cristina-Maria Cruciat, Mariann Bienz, and Christof Niehrs. Wnt Induces LRP6 Signalosomes and Promotes Dishevelled-Dependent LRP6 Phosphorylation. *Science*, 316(5831):1619–1622, June 2007.

[14] Gabriele Colozza and Bon-Kyoung Koo. Wnt/β-catenin signaling: Structure, assembly and endocytosis of the signalosome. *Development, Growth & Differentiation*, 63(3):199–218, April 2021.

[15] Eek-hoon Jho, Tong Zhang, Claire Domon, Choun-Ki Joo, Jean-Noel Freund, and Frank Costantini. Wnt/β-Catenin/Tcf Signaling Induces the Transcription of Axin2, a Negative Regulator of the Signaling Pathway. *Molecular and Cellular Biology*, 22(4):1172–1183, February 2002.

[16] Christof Niehrs and Jinlong Shen. Regulation of Lrp6 phosphorylation. *Cellular and Molecular Life Sciences*, 67(15):2551–2562, August 2010.

[17] Xiaomo Jiang and Feng Cong. Novel Regulation of Wnt Signaling at the Proximal Membrane Level. *Trends in Biochemical Sciences*, 41(9):773–783, September 2016.

[18] Bo Lu and Feng Cong. The E3 ubiquitin ligase ZNRF3 restricts WNT receptor complex activity by stimulating the selective degradation of WNT-engaged FZD. *Science Signaling*, 18(908):eadv1529, October 2025.

[19] Madelon M. Maurice and Stephane Angers. Mechanistic insights into Wnt–β-catenin pathway activation and signal transduction. *Nature Reviews Molecular Cell Biology*, 26(5):371–388, May 2025.

[20] Qiang Feng and Nan Gao. Keeping Wnt Signalosome in Check by Vesicular Traffic. *Journal of Cellular Physiology*, 230(6):1170–1180, June 2015.

[21] Lucy Brunt and Steffen Scholpp. The function of endocytosis in Wnt signaling. *Cellular and Molecular Life Sciences*, 75(5):785–795, 2018.

[22] Nydia Tejeda-Muñoz, Grace Binder, and Kuo-Ching Mei. Emerging therapeutic strategies for Wnt-dependent colon cancer targeting macropinocytosis. *Cells & Development*, 180:203974, December 2024.

[23] Ellen Youngsoo Rim, Leigh Katherine Kinney, and Roeland Nusse. β-catenin-mediated Wnt signal transduction proceeds through an endocytosis-independent mechanism. *Molecular Biology of the Cell*, 31(13):1425–1436, June 2020.

[24] Heather Hartmann, Ghalia Saad Siddiqui, Jamal Bryant, David J. Robbins, Vivian L. Weiss, Yashi Ahmed, and Ethan Lee. Wnt signalosomes: What we know that we do not know. *Bioessays*, 47(2):2400110, February 2025.

[25] Huai-Xiang Hao, Yang Xie, Yue Zhang, Olga Charlat, Emma Oster, Monika Avello, Hong Lei, Craig Mickanin, Dong Liu, Heinz Ruffner, Xiaohong Mao, Qicheng Ma, Raffaella Zamponi, Tewis Bouwmeester, Peter M. Finan, Marc W. Kirschner, Jeffery A. Porter, Fabrizio C. Serluca, and Feng Cong. ZNRF3 promotes Wnt receptor turnover in an R-spondin-sensitive manner. *Nature*, 485(7397):195–200, April 2012.

[26] Xiaomo Jiang, Olga Charlat, Raffaella Zamponi, Yi Yang, and Feng Cong. Dishevelled Promotes Wnt Receptor Degradation through Recruitment of ZNRF3/RNF43 E3 Ubiquitin Ligases. *Molecular Cell*, 58(3):522–533, May 2015.

[27] Shanshan Li, Jiahui Niu, and Ron Smits. RNF43 and ZNRF3: Versatile regulators at the membrane and their role in cancer. *Biochimica et Biophysica Acta (BBA) - Reviews on Cancer*, 1879(6):189217, November 2024.

[28] Dong Luo, Jing Zheng, Shuning Lv, Ren Sheng, Maorong Chen, Xi He, and Xinjun Zhang. Wnt induces FZD5/8 endocytosis and degradation and the involvement of RSPO-ZNRF3/RNF43 and DVL. *bioRxiv*, page 2024.10.18.619000, June 2025.

[29] Hideki Yamamoto and Hideyuki Komekado. Caveolin Is Necessary for Wnt-3a-Dependent Internalization of LRP6 and Accumulation of b-Catenin. pages 213–223, 2006.

[30] Kubilay Demir, Nadine Kirsch, Carlo A. Beretta, Gerrit Erdmann, Dierk Ingelfinger, Enrico Moro, Francesco Argenton, Matthias Carl, Christof Niehrs, and Michael Boutros. RAB8B is required for activity and caveolar endocytosis of LRP6. *Cell Reports*, 4(6):1224–1234, September 2013.

[31] Ren Sheng, Hyunjoon Kim, Hyeyoon Lee, Yao Xin, Yong Chen, Wen Tian, Yang Cui, Jong-Cheol Choi, Junsang Doh, Jin-Kwan Han, and Wonhwa Cho. Cholesterol selectively activates canonical Wnt signalling over non-canonical Wnt signalling. *Nature Communications*, 5:4393, July 2014.

[32] Alfredo Erazo-Oliveras, Mónica Muñoz-Vega, Mohamed Mlih, Venkataramana Thiriveedi, Michael L. Salinas, Jaileen M. Rivera-Rodríguez, Eunjoo Kim, Rachel C. Wright, Xiaoli Wang, Kerstin K. Landrock, Jennifer S. Goldsby, Destiny A. Mullens, Jatin Roper, Jason Karpac, and Robert S. Chapkin. Mutant APC reshapes Wnt signaling plasma membrane nanodomains by altering cholesterol levels via oncogenic β-catenin. *Nature Communications*, 14(1):4342, July 2023.

[33] Gianni M. Di Guglielmo, Christine Le Roy, Anne F. Goodfellow, and Jeffrey L. Wrana. Distinct endocytic pathways regulate TGF-β receptor signalling and turnover. *Nature Cell Biology*, 5(5):410–421, May 2003.

[34] Sun-Cheol Choi, Gun-Hwa Kim, Seung Joon Lee, Eunjoo Park, Chang-Yeol Yeo, and Jin-Kwan Han. Regulation of activin/nodal signaling by Rap2-directed receptor trafficking. *Developmental Cell*, 15(1):49–61, July 2008.

[35] Mark Von Zastrow and Alexander Sorkin. Mechanisms for Regulating and Organizing Receptor Signaling by Endocytosis. *Annual Review of Biochemistry*, 90(1):709–737, June 2021.

[36] Robert G. Parton and Mark T. Howes. Revisiting caveolin trafficking: The end of the caveosome. *The Journal of Cell Biology*, 191(3):439–441, November 2010.

[37] Lai Kuan Goh and Alexander Sorkin. Endocytosis of Receptor Tyrosine Kinases. *Cold Spring Harbor Perspectives in Biology*, 5(5):a017459, January 2013.

[38] Roshanak Irannejad, Nikoleta G. Tsvetanova, Braden T. Lobingier, and Mark von Zastrow. Effects of endocytosis on receptor-mediated signaling. *Current Opinion in Cell Biology*, 35:137–143, August 2015.

[39] Martin Baumdick, Yannick Brüggemann, Malte Schmick, Georgia Xouri, Ola Sabet, Lloyd Davis, Jason W Chin, and Philippe IH Bastiaens. EGF-dependent re-routing of vesicular recycling switches spontaneous phosphorylation suppression to EGFR signaling. *eLife*, 4:e12223, November 2015.

[40] Gabriele Colozza, Yasaman Jami-Alahmadi, Alyssa Dsouza, Nydia Tejeda-Muñoz, Lauren V. Albrecht, Eric A. Sosa, James A. Wohlschlegel, and Edward M. De Robertis. Wnt-inducible Lrp6-APEX2 interacting proteins identify ESCRT machinery and Trk-fused gene as components of the Wnt signaling pathway. *Scientific Reports*, 10:21555, December 2020.

[41] Fiete Haack, Kai Budde, and Adelinde M. Uhrmacher. Exploring the mechanistic and temporal regulation of LRP6 endocytosis in canonical WNT signaling. *Journal of Cell Science*, 133(15):jcs243675, August 2020.

[42] Saskia MA de Man, Gooitzen Zwanenburg, Tanne van der Wal, Mark A Hink, and Renée van Amerongen. Quantitative live-cell imaging and computational modeling shed new light on endogenous WNT/CTNNB1 signaling dynamics. *eLife*, 10:e66440, June 2021.

[43] Bethan Lloyd-Lewis, Alexander G. Fletcher, Trevor C. Dale, and Helen M. Byrne. Toward a quantitative understanding of the Wnt/ β -catenin pathway through simulation and experiment. *Wiley Interdisciplinary Reviews: Systems Biology and Medicine*, 5(4):391–407, July 2013.

[44] Kai Budde, Jacob Smith, Pia Wilsdorf, Fiete Haack, and Adelinde M Uhrmacher. Relating simulation studies by provenance—developing a family of wnt signaling models. *PLOS Computational Biology*, 17(8):e1009227, 2021.

[45] Mohammad Fallahi-Sichani and Jennifer J Linderman. Lipid Raft-Mediated Regulation of G-Protein Coupled Receptor Signaling by Ligands which Influence Receptor Dimerization: A Computational Study. *PLoS ONE*, 4(8):e6604–e6604, 2009.

[46] Luis S. Mayorga, Ignacio Cebrian, Meghna Verma, Stefan Hoops, and Josep Bassaganya-Riera. Reconstruction of endosomal organization and function by a combination of ODE and agent-based modeling strategies. *Biology Direct*, 13(1):1–21, December 2018.

[47] Fiete Haack, Heiko Lemcke, Roland Ewald, Tareck Rharass, and Adelinde M. Uhrmacher. Spatio-temporal Model of Endogenous ROS and Raft-Dependent WNT/Beta-Catenin Signaling Driving Cell Fate Commitment in Human Neural Progenitor Cells. *PLOS Computational Biology*, 11(3):e1004106, March 2015.

[48] Fiete Haack, Till Köster, and Adelinde M. Uhrmacher. Receptor/Raft Ratio Is a Determinant for LRP6 Phosphorylation and WNT/β-Catenin Signaling. *Frontiers in Cell and Developmental Biology*, 9, 2021.

[49] Carsten Maus, Stefan Rybacki, and Adelinde M Uhrmacher. Rule-based multi-level modeling of cell biological systems. *BMC systems biology*, 5(1):166, 2011.

[50] Tobias Helms, Tom Warnke, Carsten Maus, and Adelinde M Uhrmacher. Semantics and efficient simulation algorithms of an expressive multilevel modeling language. *ACM Transactions on Modeling and Computer Simulation (TOMACS)*, 27(2):1–25, 2017.

[51] Till Köster, Philipp Henning, Tom Warnke, and Adelinde Uhrmacher. Expressive rule-based modeling and fast simulation for dynamic compartments. *Plos one*, 19(10):e0312813, 2024.

[52] Eric Bourhis, Christine Tam, Yvonne Franke, J. Fernando Bazan, James Ernst, Jiyoung Hwang, Mike Costa, Andrea G. Cochran, and Rami N. Hannoush. Reconstitution of a Frizzled8·Wnt3a·LRP6 Signaling Complex Reveals Multiple Wnt and Dkk1 Binding Sites on LRP6. *Journal of Biological Chemistry*, 285(12):9172–9179, March 2010.

[53] Jacomijn P. Dijksterhuis, Bolormaa Baljinnyam, Karen Stanger, Hakki O. Sercan, Yun Ji, Osler Andres, Jeffrey S. Rubin, Rami N. Hannoush, and Gunnar Schulte. Systematic Mapping of WNT-FZD Protein Interactions Reveals Functional Selectivity by Distinct WNT-FZD Pairs *. *Journal of Biological Chemistry*, 290(11):6789–6798, March 2015.

[54] Yue Hua, Yilin Yang, Qian Li, Xinyu He, Wei Zhu, Jiyong Wang, and Xiaoqing Gan. Oligomerization of Frizzled and LRP5/6 protein initiates intracellular signaling for the canonical WNT/β-catenin pathway. *The Journal of Biological Chemistry*, 293(51):19710–19724, December 2018.

[55] Zachary J DeBruine, H E Xu, and Karsten Melcher. Assembly and architecture of the Wnt/β-catenin signalosome at the membrane. *British Journal of Pharmacology*, 174(24):4564–4574, 2017.

[56] Melissa V. Gammons, Trevor J. Rutherford, Zachary Steinhart, Stephane Angers, and Mariann Bienz. Essential role of the Dishevelled DEP domain in a Wnt-dependent human-cell-based complementation assay. *Journal of Cell Science*, 129(20):3892–3902, October 2016.

[57] Jacob P. Mahoney, Elise S. Bruguera, Mansi Vasishtha, Lauren B. Killingsworth, Saw Kyaw, and William I. Weis. PI(4,5)P2-stimulated positive feedback drives the recruitment of Dishevelled to Frizzled in Wnt–β-catenin signaling. *Science Signaling*, 15(748):eabo2820, August 2022.

[58] Xin Zeng, He Huang, Keiko Tamai, Xinjun Zhang, Yuko Harada, Chika Yokota, Karla Almeida, Jianbo Wang, Brad Doble, Jim Woodgett, Anthony Wynshaw-Boris, Jen-Chieh Hsieh, and Xi He. Initiation of Wnt signaling: Control of Wnt coreceptor Lrp6 phosphorylation/activation via frizzled, dishevelled and axin functions. *Development*, 135(2):367–375, January 2008.

[59] Ciara Metcalfe, Carolina Mendoza-Topaz, Juliusz Mieszczanek, and Mariann Bienz. Stability elements in the LRP6 cytoplasmic tail confer efficient signalling upon DIX-dependent polymerization. *Journal of Cell Science*, 123(9):1588–1599, May 2010.

[60] H. Sakane, H. Yamamoto, and A. Kikuchi. LRP6 is internalized by Dkk1 to suppress its phosphorylation in the lipid raft and is recycled for reuse. *Journal of Cell Science*, 123(3):360–368, January 2010.

[61] Günes Özhan, Erdinc Sezgin, Daniel Wehner, Astrid S Pfister, Susanne J Kühl, Birgit Kagermeier-Schenk, Michael Kühl, Petra Schwille,

and Gilbert Weidinger. Lypd6 enhances Wnt/β-catenin signaling by promoting Lrp6 phosphorylation in raft plasma membrane domains. *Developmental cell*, 26(4):331–345, August 2013.

[62] Birgit Kagermeier-Schenk, Daniel Wehner, Günes Özhan-Kizil, Hideki Yamamoto, Jian Li, Katharina Kirchner, Christian Hoffmann, Peter Stern, Akira Kikuchi, Alexandra Schambony, and Gilbert Weidinger. Waif1/5T4 Inhibits Wnt/β-Catenin Signaling and Activates Noncanonical Wnt Pathways by Modifying LRP6 Subcellular Localization. *Developmental Cell*, 21(6):1129–1143, December 2011.

[63] Carsten Maus, Stefan Rybacki, and Adelinde M. Uhrmacher. Rule-based multi-level modeling of cell biological systems. *BMC Systems Biology*, 5(1):166, October 2011.

[64] Tobias Helms, Tom Warnke, Carsten Maus, and Adelinde M. Uhrmacher. Semantics and Efficient Simulation Algorithms of an Expressive Multilevel Modeling Language. *ACM Transactions on Modeling and Computer Simulation*, 27(2):8:1–8:25, May 2017.

[65] Gunnar Schulte. Frizzleds and WNT/β-catenin signaling – The black box of ligand–receptor selectivity, complex stoichiometry and activation kinetics. *European Journal of Pharmacology*, 763:191–195, September 2015.

[66] Erdinc Sezgin, Yagmur Azbazdar, Xue W. Ng, Cathleen Teh, Kai Simons, Gilbert Weidinger, Thorsten Wohland, Christian Eggeling, and Gunes Ozhan. Binding of canonical Wnt ligands to their receptor complexes occurs in ordered plasma membrane environments. *The Febs Journal*, 284(15):2513–2526, August 2017.

[67] Yagmur Azbazdar, Ozgun Ozalp, Erdinc Sezgin, Sapthaswaran Veerapathiran, Anna L. Duncan, Mark S. P. Sansom, Christian Eggeling, Thorsten Wohland, Ezgi Karaca, and Gunes Ozhan. More Favorable Palmitic Acid Over Palmitoleic Acid Modification of Wnt3 Ensures Its Localization and Activity in Plasma Membrane Domains. *Frontiers in Cell and Developmental Biology*, 7, 2019.

[68] Jinxiao Chen, Hongwei Yan, Dan-ni Ren, Yan Yin, Zhi Li, Qingqing He, Da Wo, Margaret Su-chun Ho, Yihan Chen, Zhongmin Liu, Jianhua Yang, Shangfeng Liu, and Weidong Zhu. LRP6 dimerization through its LDLR domain is required for robust canonical Wnt pathway activation. *Cellular Signalling*, 26(5):1068–1074, May 2014.

[69] Meritxell Vinyoles, Beatriz Del Valle-Pérez, Josué Curto, Rosa Viñas-Castells, Lorena Alba-Castellón, Antonio García de Herreros, and Mireia Duñach. Multivesicular GSK3 Sequestration upon Wnt Signaling Is Controlled by p120-Catenin/Cadherin Interaction with LRP5/6. *Molecular Cell*, 53(3):444–457, February 2014.

[70] Wenyan Lu, Chia-Chen Liu, Jaideep V. Thottassery, Guojun Bu, and Yonghe Li. Mesd is a universal inhibitor of Wnt coreceptors LRP5 and LRP6 and blocks Wnt/beta-catenin signaling in cancer cells. *Biochemistry*, 49(22):4635–4643, June 2010.

[71] Chia-Chen Liu, Takahisa Kanekiyo, Barbara Roth, and Guojun Bu. Tyrosine-based Signal Mediates LRP6 Receptor Endocytosis and Desensitization of Wnt/β-Catenin Pathway Signaling. *Journal of Biological Chemistry*, 289(40):27562–27570, March 2014.

[72] Zahid Khan, Sapna Vijayakumar, Teresa Villanueva de la Torre, Sabrina Rotolo, and Anna Bafico. Analysis of Endogenous LRP6 Function Reveals a Novel Feedback Mechanism by Which Wnt Negatively Regulates Its Receptor. *Molecular and Cellular Biology*, 27(20):7291–7301, 2007.

[73] Thomas Schwarz-Romond, Ciara Metcalfe, and Mariann Bienz. Dynamic recruitment of axin by Dishevelled protein assemblies. *Journal of Cell Science*, 120(14):2402–2412, July 2007.

[74] Takahiro Fujiwara, Ken Ritchie, Hideji Murakoshi, Ken Jacobson, and Akihiro Kusumi. Phospholipids undergo hop diffusion in compartmentalized cell membrane. *The Journal of Cell Biology*, 157(6):1071–1082, 2002.

[75] Khuloud Jaqaman and Sergio Grinstein. Regulation from within: The cytoskeleton in transmembrane signaling. *Trends in cell biology*, 22(10):515–526, October 2012.

[76] Takahiro K. Fujiwara, Kokoro Iwasawa, Ziya Kalay, Taka A. Tsunoyama, Yusuke Watanabe, Yasuhiro M. Umemura, Hideji Murakoshi, Kenichi G. N. Suzuki, Yuri L. Nemoto, Nobuhiro Morone, and Akihiro Kusumi. Confined diffusion of transmembrane proteins and lipids induced by the same actin meshwork lining the plasma membrane. *Molecular Biology of the Cell*, 27(7):1101–1119, April 2016.

[77] Ron Milo and Rob Phillips. *Cell Biology by the Numbers*. Garland Science, New York, December 2015.

[78] Jan Hendrik Voss, Zsombor Koszegi, Yining Yan, Emily Shorter, Lukas Grätz, Johanna T. Lanner, Davide Calebiro, and Gunnar Schulte. WNT-induced association of Frizzled and LRP6 is not sufficient for the initiation of WNT/β-catenin signaling. *Nature Communications*, 16(1):4848, May 2025.

[79] Falk Schneider, Dominic Waithe, Mathias P. Clausen, Silvia Galiani, Thomas Koller, Gunes Ozhan, Christian Eggeling, and Erdinc Sezgin. Diffusion of lipids and GPI-anchored proteins in actin-free plasma membrane vesicles measured by STED-FCS. *Molecular Biology of the Cell*, 28(11):1507–1518, June 2017.

[80] Akihiro Kusumi, Takahiro K. Fujiwara, Rahul Chadda, Min Xie, Taka A. Tsunoyama, Ziya Kalay, Rinshi S. Kasai, and Kenichi G.N. Suzuki. Dynamic Organizing Principles of the Plasma Membrane that Regulate Signal Transduction: Commemorating the Fortieth Anniversary of Singer and Nicolson's Fluid-Mosaic Model. *Annual Review of Cell and Developmental Biology*, 28(1):215–250, 2012.

[81] Ken Jacobson, Ping Liu, and B. Christoffer Lagerholm. The Lateral Organization and Mobility of Plasma Membrane Components. *Cell*, 177(4):806–819, May 2019.

[82] Suvrajit Saha, Anupama Ambika Anilkumar, and Satyajit Mayor. GPI-anchored protein organization and dynamics at the cell surface. *Journal of Lipid Research*, 57(2):159–175, February 2016.

[83] Sara Sigismund, Elisabetta Argenzio, Daniela Tosoni, Elena Cavallaro, Simona Polo, and Pier Paolo Di Fiore. Clathrin-Mediated Internalization Is Essential for Sustained EGFR Signaling but Dispensable for Degradation. *Developmental Cell*, 15(2):209–219, August 2008.

[84] Nagaja Capitani and Cosima T. Baldari. F-Actin Dynamics in the Regulation of Endosomal Recycling and Immune Synapse Assembly. *Frontiers in Cell and Developmental Biology*, 9:670882, 2021.

[85] Tirthadipa Pradhan-Sundd and Esther M. Verheyen. The Myopic-Ubpy-Hrs nexus enables endosomal recycling of Frizzled. *Molecular Biology of the Cell*, 26(18):3329–3342, September 2015.

[86] Jun Fan, Maria Sammalkorpi, and Mikko Haataja. Formation and regulation of lipid microdomains in cell membranes: Theory, modeling, and speculation. *FEBS Letters*, 584(9):1678–1684, May 2010.

[87] Blanca B. Diaz-Rohrer, Kandice R. Levental, Kai Simons, and Ilya Levental. Membrane raft association is a determinant of plasma membrane localization. *Proceedings of the National Academy of Sciences*, 111(23):8500–8505, October 2014.

[88] Barbara Diaz-Rohrer, Ivan Castello-Serrano, Sze Ham Chan, Hong-Yin Wang, Carolyn R. Shurer, Kandice R. Levental, and Ilya Levental. Rab3 mediates a pathway for endocytic sorting and plasma membrane recycling of ordered microdomains. *Proceedings of the National Academy of Sciences*, 120(10):e2207461120, March 2023.

[89] Jan P. Gerlach, Ingrid Jordens, Daniele V. F. Tauriello, Ineke van 't Land-Kuper, Jeroen M. Bugter, Ivar Noordstra, Johanneke van der Kooij, Teck Y. Low, Felipe X. Pimentel-Muiños, Despina Xanthakis, Nicola Fenderico, Catherine Rabouille, Albert J. R. Heck, David A. Egan, and Madelon M. Maurice. TMEM59 potentiates Wnt signaling by promoting signalosome formation. *Proceedings of the National Academy of Sciences*, 115(17):E3996–E4005, April 2018.

[90] Blanca Diaz-Rohrer, Kandice R. Levental, and Ilya Levental. Rafting through traffic: Membrane domains in cellular logistics. *Biochimica et Biophysica Acta (BBA) - Biomembranes*, 1838(12):3003–3013, December 2014.

[91] Qing Chen, Yi Su, Janine Wesslowski, Anja I Hagemann, Mirana Ramialison, Joachim Wittbrodt, Steffen Scholpp, and Gary Davidson. Tyrosine phosphorylation of LRP6 by Src and Fer inhibits Wnt/β-catenin signalling. *EMBO reports*, 15(12):1254–1267, December 2014.

[92] Caspar T. H. Jonker, Claire Deo, Patrick J. Zager, Ariana N. Tkachuk, Alan M. Weinstein, Enrique Rodriguez-Boulan, Luke D. Lavis, and Ryan Schreiner. Accurate measurement of fast endocytic recycling kinetics in real time. *Journal of Cell Science*, 133(2):jcs231225, January 2020.

[93] Jiachao Xu, Yu Liang, Nan Li, Song Dang, Amin Jiang, Yiqun Liu, Yuting Guo, Xiaoyu Yang, Yi Yuan, Xinyi Zhang, Yaran Yang, Yongtao Du, Anbing Shi, Xiaoyun Liu, Dong Li, and Kangmin He. Clathrin-associated carriers enable recycling through a kiss-and-run mechanism. *Nature Cell Biology*, 26(10):1652–1668, October 2024.

[94] Catriona Y. Logan and Roel Nusse. The Wnt Signaling Pathway in Development and Disease. *Annual Review of Cell and Developmental Biology*, 20(1):781–810, 2004.

[95] Rene Jackstadt, Michael Charles Hodder, and Owen James Sansom. WNT and β-Catenin in Cancer: Genes and Therapy. *Annual Review of Cancer Biology*, 4(Volume 4, 2020):177–196, March 2020.

[96] Lena Cibulski, Fiete Haack, Adelinde Uhrmacher, and Stefan Bruckner. Visual Analysis of Time-Dependent Observables in Cell Signaling Simulations. *Eurographics Workshop on Visual Computing for Biology and Medicine*, 2025.

[97] Ethan Lee, Adrian Salic, Roland Krüger, Reinhart Heinrich, and Marc W Kirschner. The Roles of APC and Axin Derived from Experimental and Theoretical Analysis of the Wnt Pathway. *PLoS Biol*, 1(1):e10, October 2003.

[98] Ofelia Tacchelly-Benites, Zhenghan Wang, Eungi Yang, Hassina Benchabane, Ai Tian, Michael P. Randall, and Yashi Ahmed. Axin phosphorylation in both Wnt-off and Wnt-on states requires the tumor suppressor APC. *PLOS Genetics*, 14(2):e1007178, February 2018.

[99] Nicholas S. Tolwinski and Eric Wieschaus. Rethinking WNT signaling. *Trends in genetics: TIG*, 20(4):177–181, April 2004.

[100] Bryan T. MacDonald and Xi He. Frizzled and LRP5/6 Receptors for Wnt/β-Catenin Signaling. *Cold Spring Harbor Perspectives in Biology*, 4(12):a007880, December 2012.

[101] Ian V. Chia and Frank Costantini. Mouse Axin and Axin2/Conductin Proteins Are Functionally Equivalent In Vivo. *Molecular and Cellular Biology*, 25(11):4371–4376, June 2005.

[102] Kwang-Hyun Cho, Songjoon Baek, and Myong-Hee Sung. Wnt pathway mutations selected by optimal beta-catenin signaling for tumorigenesis. *FEBS letters*, 580(15):3665–3670, June 2006.

[103] Christian Wawra, Michael Kühl, and Hans A. Kestler. Extended analyses of the Wnt/β-catenin pathway: Robustness and oscillatory behaviour. *FEBS Letters*, 581(21):4043–4048, August 2007.

[104] Dominic B. Bernkopf, Michel V. Hadjihannas, and Jürgen Behrens. Negative-feedback regulation of the Wnt pathway by conductin/axin2 involves insensitivity to upstream signalling. *J Cell Sci*, 128(1):33–39, January 2015.

[105] J. Mao, J. Wang, B. Liu, W. Pan, G. H. Farr, C. Flynn, H. Yuan, S. Takada, D. Kimelman, L. Li, and D. Wu. Low-density lipoprotein receptor-related protein-5 binds to Axin and regulates the canonical Wnt signaling pathway. *Molecular Cell*, 7(4):801–809, April 2001.

[106] Nicholas S Tolwinski, Marcel Wehrli, Anna Rives, Naz Erdeniz, Stephen DiNardo, and Eric Wieschaus. Wg/Wnt Signal Can Be Transmitted through Arrow/LRP5,6 and Axin Independently of Zw3/Gsk3β Activity. *Developmental Cell*, 4(3):407–418, March 2003.

[107] Matt Kofron, Bilge Birsoy, Douglas Houston, Qinghua Tao, Christopher Wylie, and Janet Heasman. Wnt11/beta-catenin signaling in both oocytes and early embryos acts through LRP6-mediated regulation of axin. *Development (Cambridge, England)*, 134(3):503–513, February 2007.

[108] Shih-Min A. Huang, Yuji M. Mishina, Shanming Liu, Atwood Cheung, Frank Stegmeier, Gregory A. Michaud, Olga Charlat, Elizabeth Wiellette, Yue Zhang, Stephanie Wiessner, Marc Hild, Xiaoying Shi, Christopher J. Wilson, Craig Mickanin, Vic Myer, Aleem Fazal, Ronald Tomlinson, Fabrizio Serluca, Wenlin Shao, Hong Cheng, Michael Shultz, Christina Rau, Markus Schirle, Judith Schlegl, Sonja Ghidelli, Stephen Fawell, Chris Lu, Daniel Curtis, Marc W. Kirschner, Christoph Lengauer, Peter M. Finan, John A. Tallarico, Tewis Bouwmeester, Jeffery A. Porter, Andreas Bauer, and Feng Cong. Tankyrase inhibition stabilizes axin and antagonizes Wnt signalling. *Nature*, 461(7264):614, October 2009.

[109] Tor Espen Thorvaldsen, Nina Marie Pedersen, Eva Maria Wenzel, and Harald Stenmark. Differential Roles of AXIN1 and AXIN2 in Tankyrase Inhibitor-Induced Formation of Degradasomes and β-Catenin Degradation. *PLOS ONE*, 12(1):e0170508, January 2017.

[110] Katharina Klement, Martina Brückner, and Dominic B. Bernkopf. Phosphorylation of axin within biomolecular condensates counteracts its tankyrase-mediated degradation. *Journal of Cell Science*, 136(20):jcs261214, October 2023.

[111] Xin Zeng, Keiko Tamai, Brad Doble, Shitao Li, He Huang, Raymond Habas, Heidi Okamura, Jim Woodgett, and Xi He. A dual-kinase mechanism for Wnt co-receptor phosphorylation and activation. *Nature*, 438(7069):873–877, December 2005.

[112] B. del Valle-Perez, O. Arques, M. Vinyoles, A. G. de Herreros, and M. Dunach. Coordinated Action of CK1 Isoforms in Canonical Wnt Signaling. *Molecular and Cellular Biology*, 31(14):2877–2888, May 2011.

[113] Rami N. Hannoush. Kinetics of Wnt-Driven β-Catenin Stabilization Revealed by Quantitative and Temporal Imaging. *PLoS ONE*, 3(10):e3498, October 2008.

[114] Kumpei Yamanishi, Marc Fiedler, Shin-ichi Terawaki, Yoshiki Higuchi, Mariann Bienz, and Naoki Shibata. A direct heterotypic interaction between the DIX domains of Dishevelled and Axin mediates signaling to β-catenin. *Science Signaling*, 12(611):eaaw5505, December 2019.

[115] Orianne Mazemondet, Mathias John, Stefan Leye, Arndt Rolfs, and Adelinde M Uhrmacher. Elucidating the Sources of beta-Catenin Dynamics in Human Neural Progenitor Cells. *PLoS ONE*, 7(8):e42792–e42792, August 2012.